Article

Omitting labor responses to heat stress underestimates future climate impact on agriculture

Supplementary Information

Di Sheng[1, *], Xin Zhao[1, *], James A. Edmonds[1], Stephanie T. Waldhoff[1], Pralit Patel[1], Brian C. O'Neill[1], Claudia Tebaldi[1], Marshall A. Wise[1]

[1]Joint Global Change Research Institute, Pacific Northwest National Laboratory, 5825 University Research Ct, College Park, MD 20740, USA.

* Corresponding Authors: Di Sheng (di.sheng@pnnl.gov) and Xin Zhao (xin.zhao@pnnl.gov)

Table of Contents

S1. Supplementary Methods

S1.1. Heat stress and labor productivity loss

The variation in crop calendars across regions and crop types suggests that labor involved in diverse crop production activities may encounter differing levels of heat stress. To capture this heterogeneous heat stress across regions and crops, we calculate crop-specific labor heat stress using weather inputs from days falling within the crop calendars.

We first map crop calendar information from the SAGE dataset[1] to GCAM crop (Table S2) and obtain country-level start and end dates for planting and harvesting activities for GCAM crop calendars. This process results in crop calendar information for 790 combinations of 131 countries and 14 GCAM crops. For crops such as winter wheat, spanning two calendar years from planting to harvesting activities, we incorporate necessary weather data from subsequent calendar years to ensure appropriate inputs for heat stress calculation. In cases where crop calendars are unavailable for specific crops in a region, we adopt the longest duration among available crop calendars in that region. Country-level crop calendar data is then extended to all grids within the respective country boundaries. The period spanning from the planting initiation to the harvesting completion is denoted as "crop days". This process generates grid-level crop calendar filters for 14 GCAM crops and 131 countries, facilitating the exclusion of daily gridded weather data falling outside of crop days from the heat stress calculation.

With the daily gridded weather inputs, including daily mean near-surface air temperature (tas), relative humidity (hurs), and air pressure (ps), during crop days, we approximate the crop-specific daily mean gridded WBGT for agricultural labor using equation (1).

$$WBGT = 0.7WBT + 0.3GT \qquad (1)$$

where WBT is the wet bulb temperature, and is calculated with the Davies-Jones method[2] in our study, and we use the 2-m reference temperature[1] (tas) as a proxy for the globe temperature (GT).

We then translate the daily gridded WBGT to daily gridded labor capacity η using equations **Error! Reference source not found.**)[3] and (3)[4] to feature a high and low labor productivity loss to WBGT (Fig. S3a), respectively.

$$\eta = 100 - 25 \cdot \max\,(0, WBGT - 25)^{2/3} \qquad (2)$$

---

[1] ISIMIP2b provides “near-surface air temperature” which refers to the air temperature at 2 meters above the ground.

$$\eta = \begin{cases} 100, & WBGT \le 26 \\ 100 - \frac{100-25}{36-26}(WBGT - 26), & 26 < WBGT \le 36 \\ 25, & WBGT > 36 \end{cases} \quad (3)$$

Labor productivity loss multiplier in future period t is calculated by dividing the future period labor capacity and the base year labor capacity η_t/η_{2015}. Agricultural production in GCAM is modeled at the water basin and annual level, so the last step is to transform the spatial and temporal resolution of daily gridded labor productivity loss multiplier to the annual water basin level.

We first conduct the temporal aggregation by averaging daily values over crop days for a given year. We then use gridded MIRCA2000 crop harvested area by irrigation practice[5] to identify grids within a water basin that have historically planted a given GCAM crop (Table S3) with a given irrigation practice, and then average across these grids to obtain the water-basin level crop and irrigation practice specific labor productivity loss multiplier. In short, grids that have not historically planted a crop are excluded from the water basin multiplier aggregation.

This transformation enables us to translate daily gridded weather data into annual water basin-level labor productivity loss multiplier for GCAM. For GCAM crops not covered by SAGE data, heat-induced labor productivity loss mirrors that of "MiscCrop". The annual water basin-level multipliers are then applied to labor input-output coefficient across crop production technology in the Reference scenario to represent the crop labor productivity under heat stress in future periods.

S1.2. Crop yield response to climate change

GEPIC is a site-based crop model while LPJmL is a global ecosystem model, and both GGCMs project actual yield under specific environmental stresses, opposite to potential yield simulated without environmental stresses. Climate inputs to GEPIC include CO2 concentration, daily minimum and maximum temperature, relative humidity, shortwave downwelling radiation, total precipitation, and near-surface wind speed. Climate inputs to LPJmL include CO2 concentration, daily mean temperature, longwave downwelling radiation, shortwave downwelling radiation, and total precipitation. We use the Osiris package[6] to map the gridded crop yield responses from ISIMIP2b with GEPIC and LPJmL into water-basin GCAM crop yield relative to the **NoCC** in GCAM. Combinations of 2 GCMs and 2 GGCMs project 4 estimates of exogenous crop yield change compared to the baseline levels in the **NoCC**. LPJmL projects an increase in global mean staple crop yield (weighted by initial land allocation) with both HadGEM2 (7%) and GFDL (10%), while GEPIC projects staple crop yield increases with GFDL (4%) and decreases with HadGEM2 (-2%). Staple crops consist of corn, rice, wheat, other grains, and root tubers.

S1.3. General GCAM description

GCAM models annual agricultural production at the intersection of 235 water basins and the 32 regions for 21 crop commodities, 6 livestock commodities, and a primary forestry product. Land use allocation is modeled by a nested logit approach, while crop yield at the technology level (i.e., by irrigation and inputs) connects cropland to production. Crop yield across technology is different due to different irrigation and management practices. Technology transition allows endogenous crop yield response at the aggregate level. The model employs a logit-based Armington approach to capture interregional trade. A calorie-based food demand structure, parameterized based on historical observations[7], is applied to model GCAM commodities demand for staple and non-staple food. Agricultural labor

For this study, we adopt the same assumptions from the Evolving scenario in Sheng et al (2024)[8] to represent regional trajectories of agricultural labor productivity growth and agricultural labor transition. The population[9] and income[10] projections are from the SSP2 "Middle-of-the-Road" scenario. Agricultural labor supply is linked to the projected rural population from SSP2 and responds to the agricultural wage rate. An economy-wide total factor productivity (TFP) is calibrated to the GDP trajectory. Biophysical crop yield growth assumptions are based on FAO projections[11,12]. Agricultural labor productivity growth is set equal to the calibrated TFP, and the global average agricultural productivity is set to more than quadruple from 2015 to 2100, with the highest productivity growth in Africa. Fig. S14 represents the agroeconomic pathways of the Evolving scenario, which serves as the NoCC experiment of this study. Increased labor productivity contributes to a 42% decrease in global agricultural employment (not including fishery) despite global agricultural output value more than doubling over the same time. While agricultural employment is projected to be continuously decreasing in most regions since 2015, agricultural employment in Africa is projected to peak around 2060 to support agricultural expansion from population growth. We implement different labor and capital intensities and crop yield outcomes across crop production technology, allowing for endogenous factor productivity responses via technology transition.

S2. Supplementary Figures

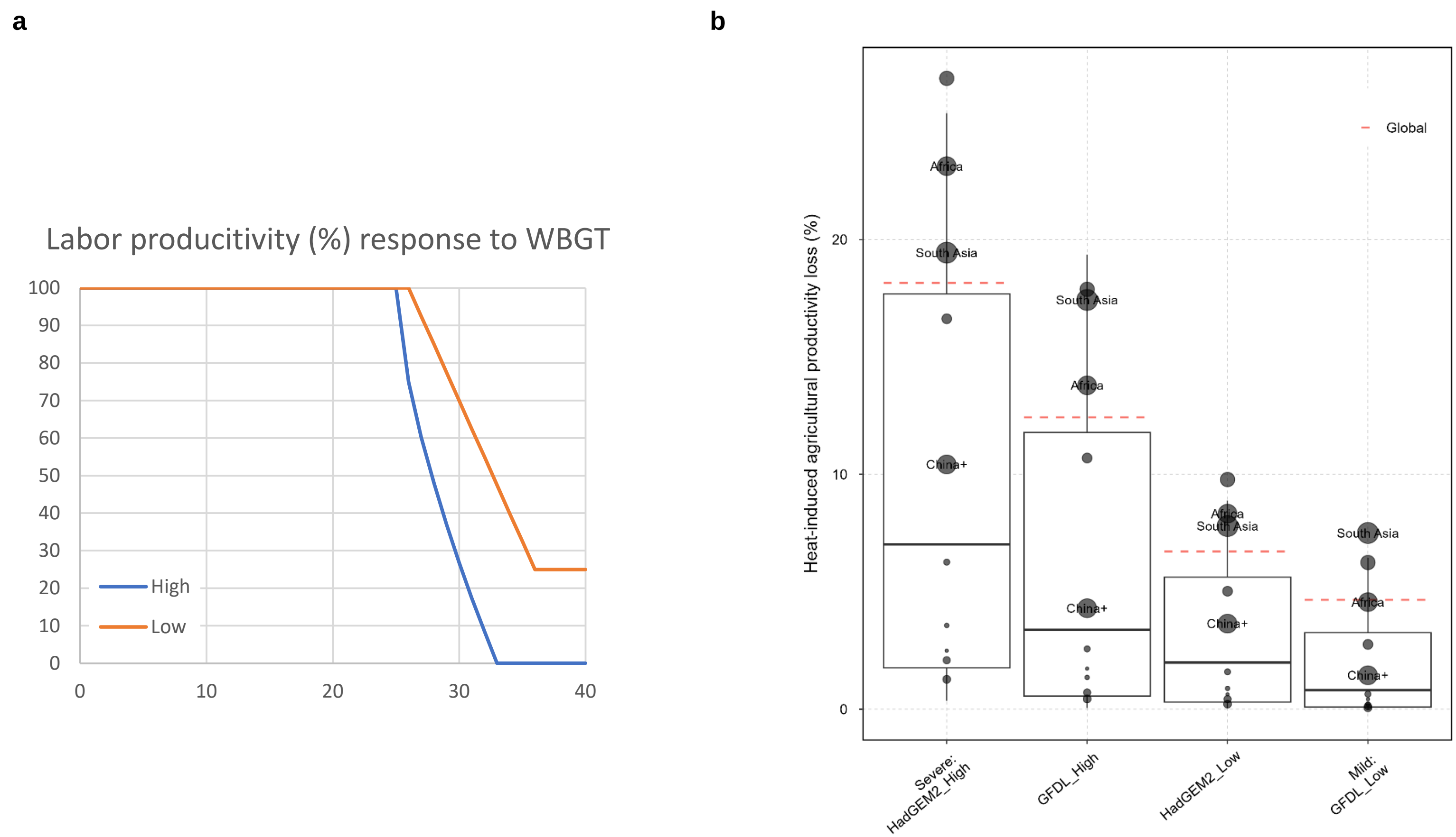

Fig. S1. Labor-heat responses. **a** shows the functional form of labor-heat response function used in this study. The high response function is from Dunne et al (2013)[3] and the low response function is from Roson and Sartori (2016)[13]. **b** shows the distributions of heat-induced labor productivity loss across all GCAM crops and 32 GCAM regions in 2100, for 4 projected heat stress scenarios. The regional aggregation is weighted by 2015 labor employment by water basins and sectors. Boxes represent the 25th percentile and 75th percentile values, whiskers denote the 5th percentile and 95th percentile values. Black solid lines denote the median, and red dashed lines denote the global means. The size of grey dots is positively associated with the regional base year agricultural employment. As regions with more severe expected heat stress have larger agricultural employment in 2015, the global means are much larger than the median, and outside of the boxes.

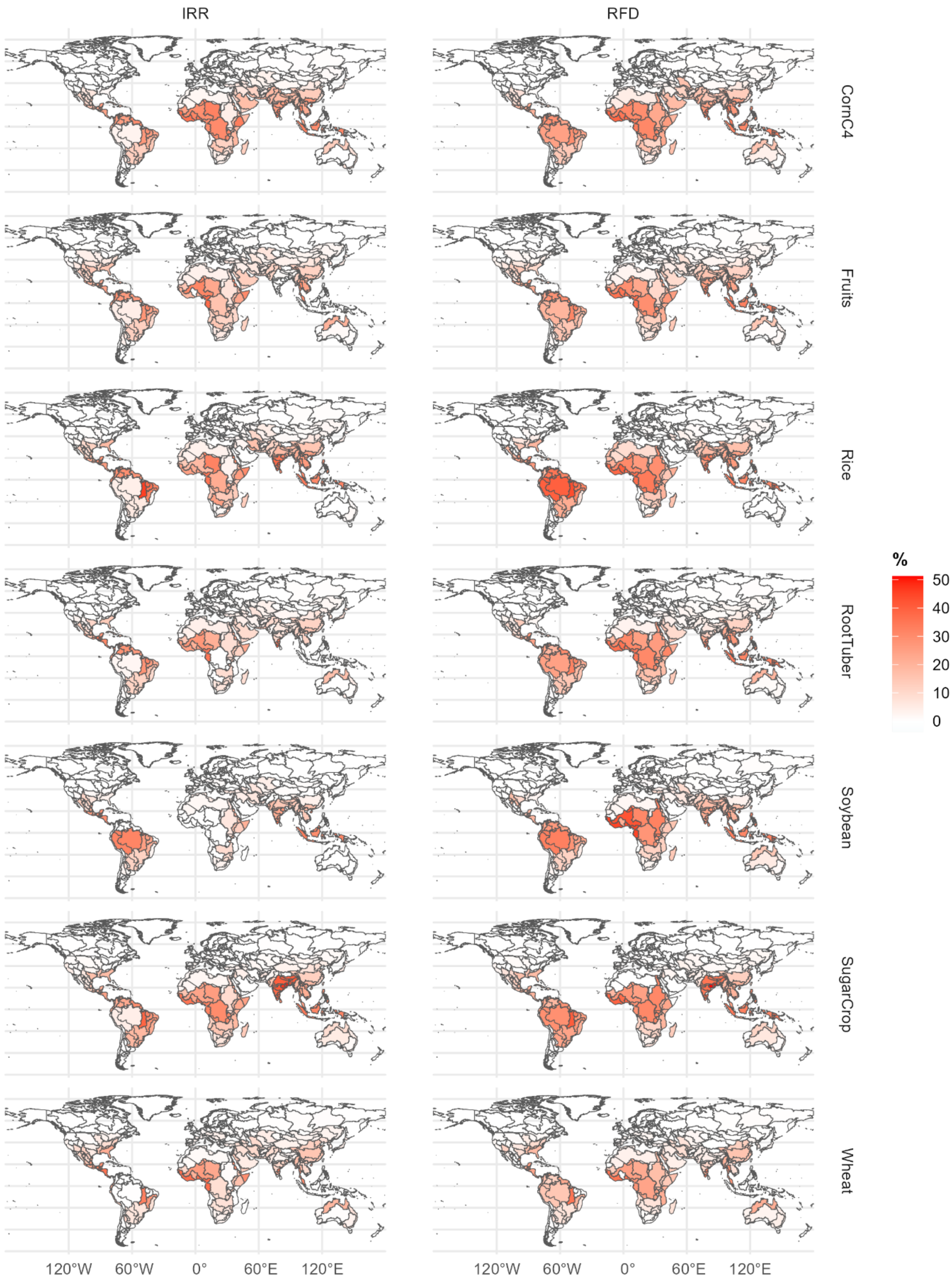

Fig. S2. Average heat-induced labor productivity loss by irrigation practice across GCAM crops at water basin level in 2100 with HadGEM2-High scenario. Weighted by labor allocation in the base year. IRR denotes irrigated, and RFD denotes rain-fed. Calculated by authors.

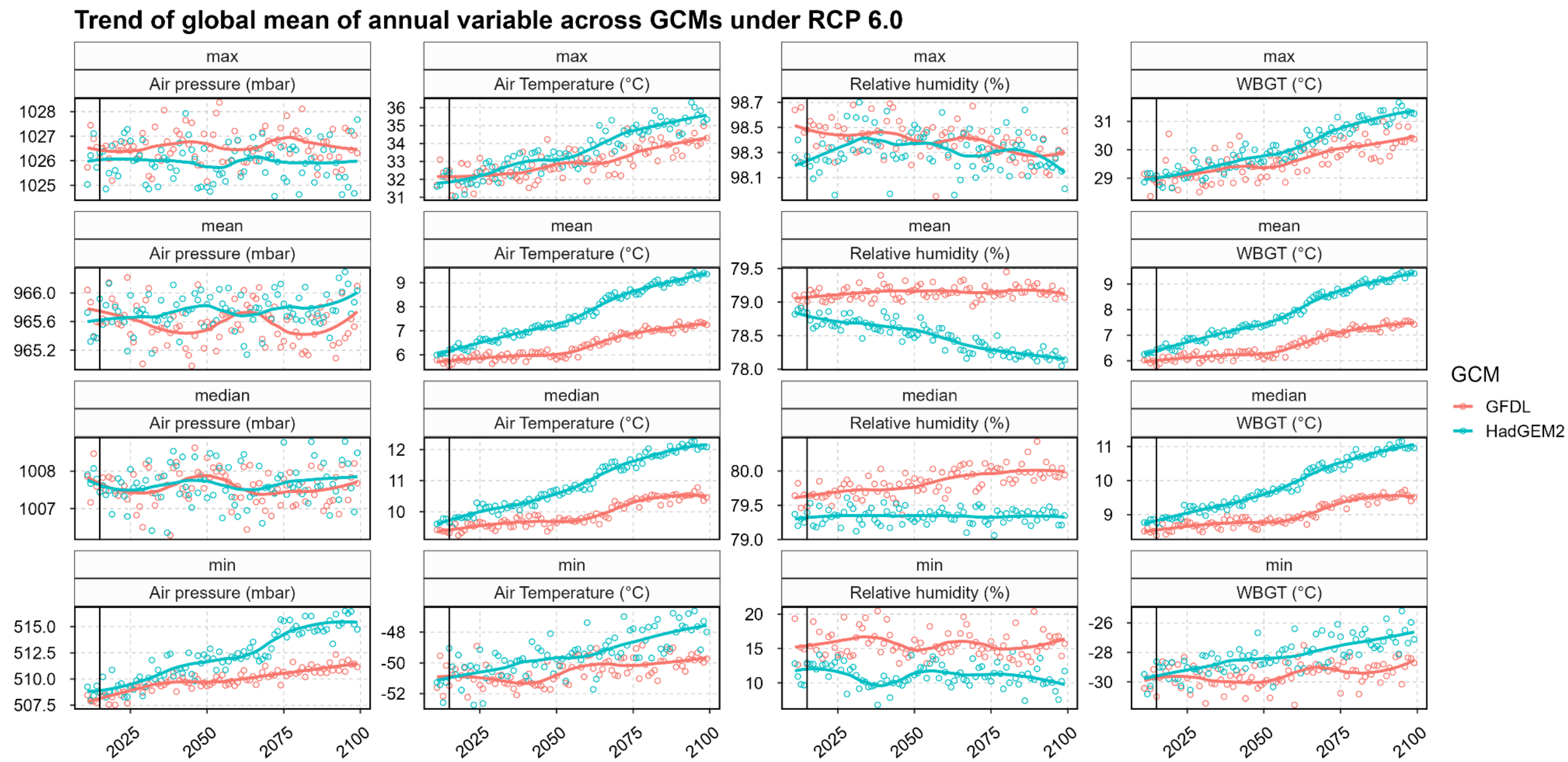

Fig. S3. Projected global annual trends of daily mean air temperature, relative humidity, and air pressure from two GCMs with RCP 6.0. Circles represent the annual mean, and the line is a loess-fitted trend with a span value of 0.5. Source: Author calculation based on the ISMIPS2b data.

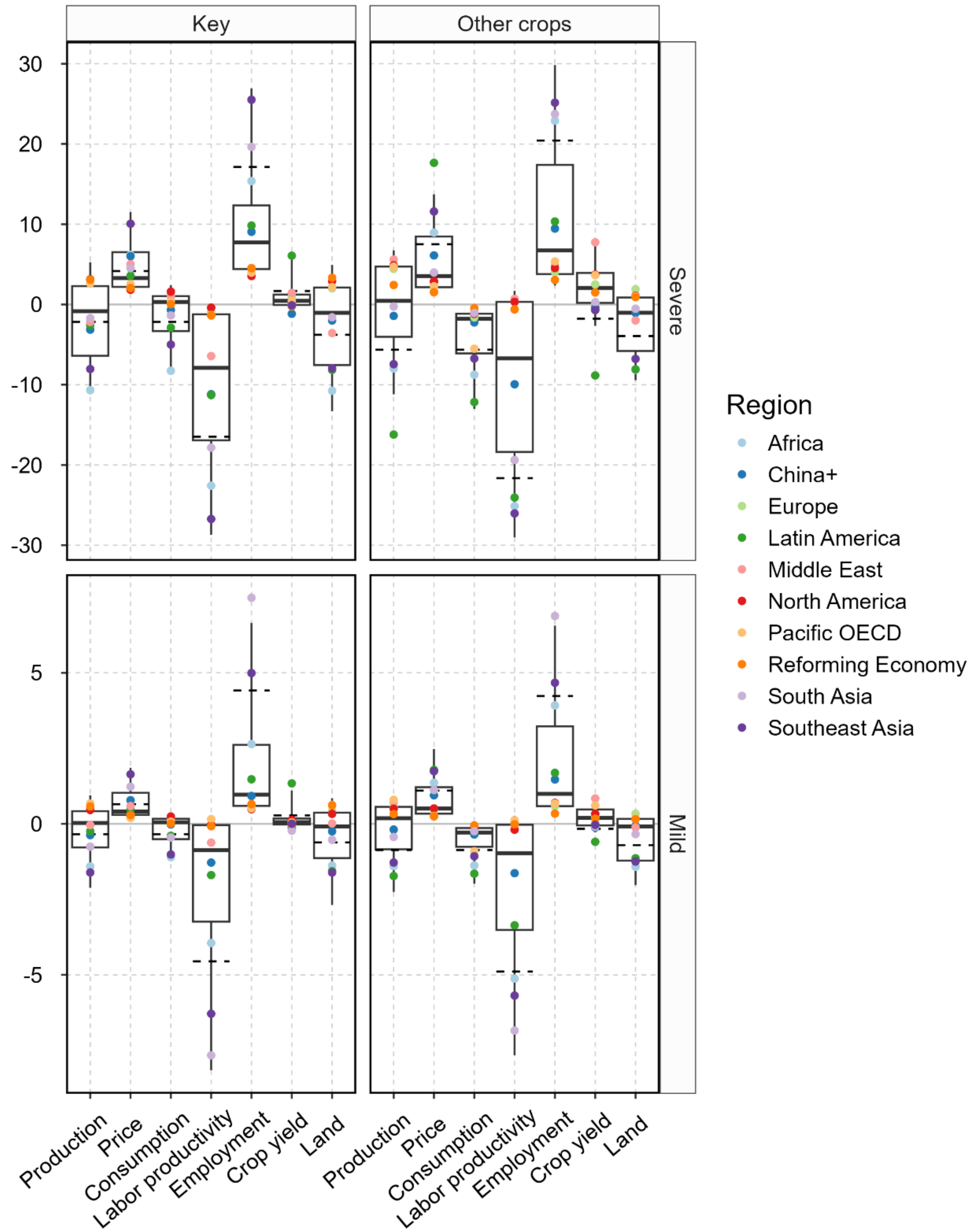

Fig. S4. Market response due to heat-induced labor productivity loss for key crops and other crops in 2100. in the Severe and Mild scenarios under RCP 6.0. Scenarios are defined with the choices of General Circulation Models-Gridded Crop Models-Labor Heat Response Models. Severe: HadGEM2-GEPIC-High, Mild: GFDL-GEPIC-Low. The black dashed lines denote the World means. Boxplot is across 32 GCAM regions by crop groups. Whiskers represent the values of the 5th to the 95th percentile; boxes range from the 25th to the 75th percentile. The thick black lines denote the medians. Color dots denote the aggregated regional means. Source: GCAM outcomes.

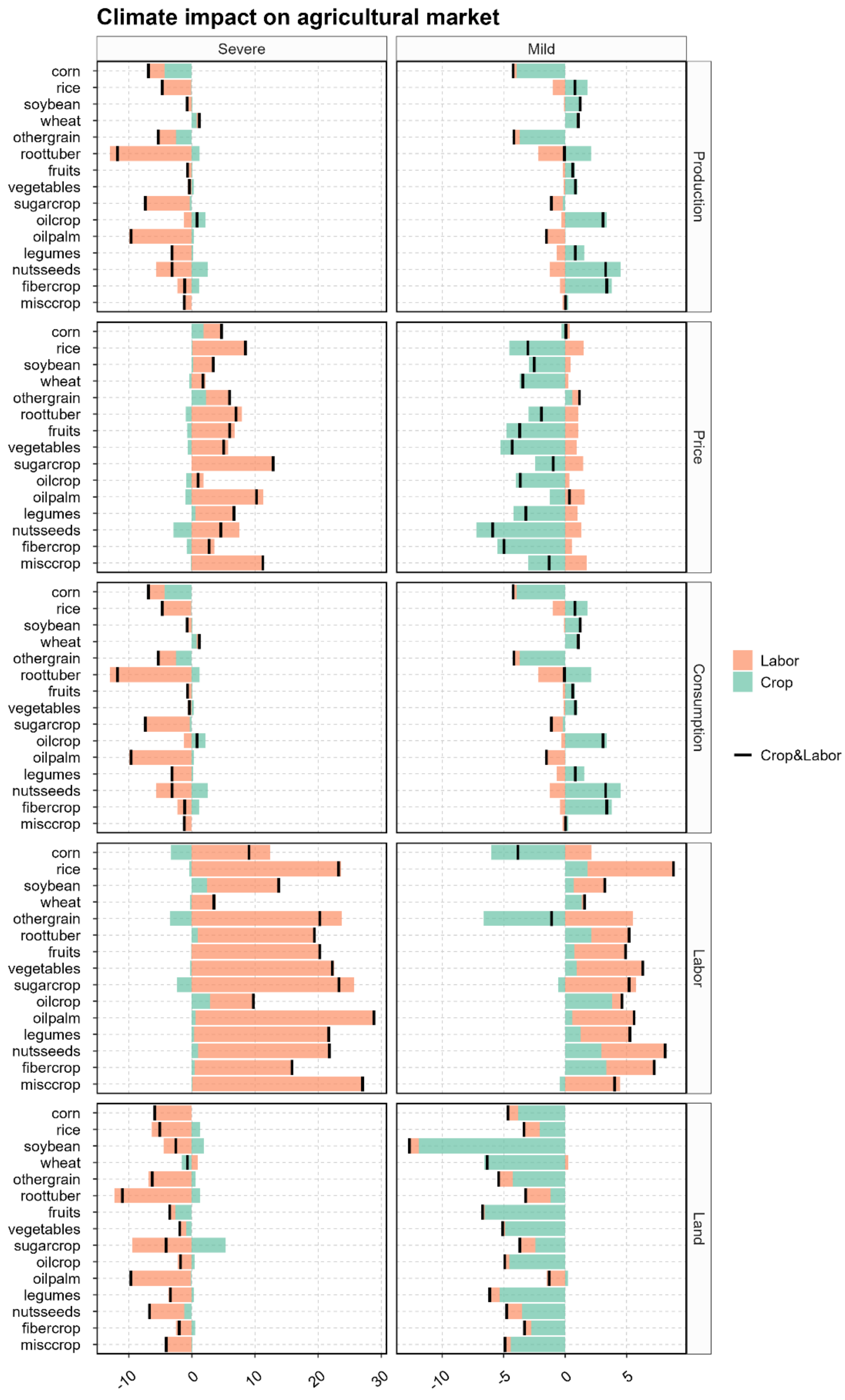

Fig. S5. Climate impact on individual crop market outcomes and production inputs in 2100 in the Severe and Mild scenarios under RCP 6.0. Scenarios are defined with the choices of General Circulation Models-Gridded Crop Models-Labor Heat Response Models. Severe: HadGEM2-GEPIC-High, Mild: GFDL-GEPIC-Low. Source: GCAM outcomes.

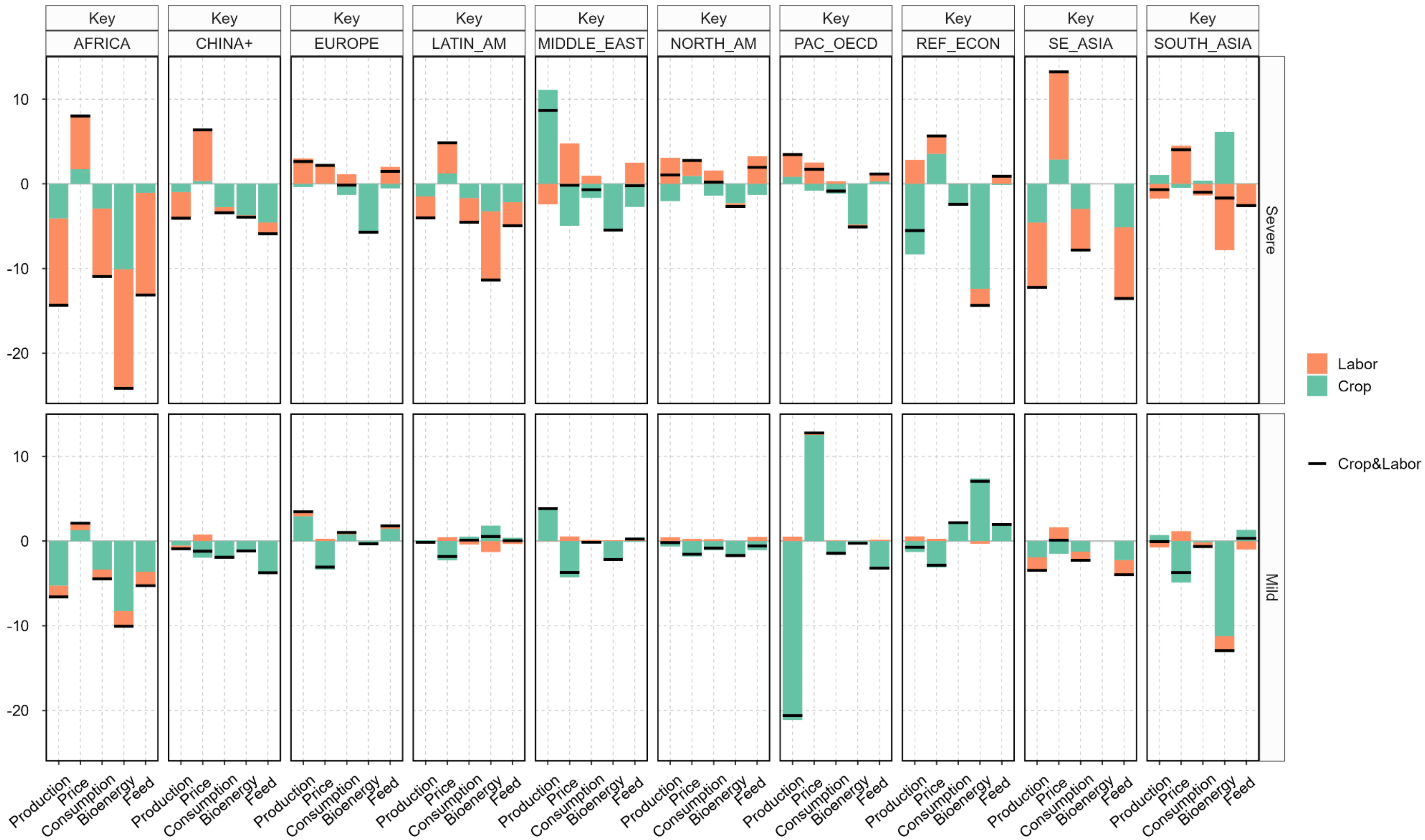

Fig. S6. Climate impact on regional key crops market outcomes in 2100 in the Severe and Mild scenarios under RCP 6.0. Scenarios are defined with the choices of General Circulation Models-Gridded Crop Models-Labor Heat Response Models. Severe: HadGEM2-GEPIC-High, Mild: GFDL-GEPIC-Low. Source: GCAM outcomes.

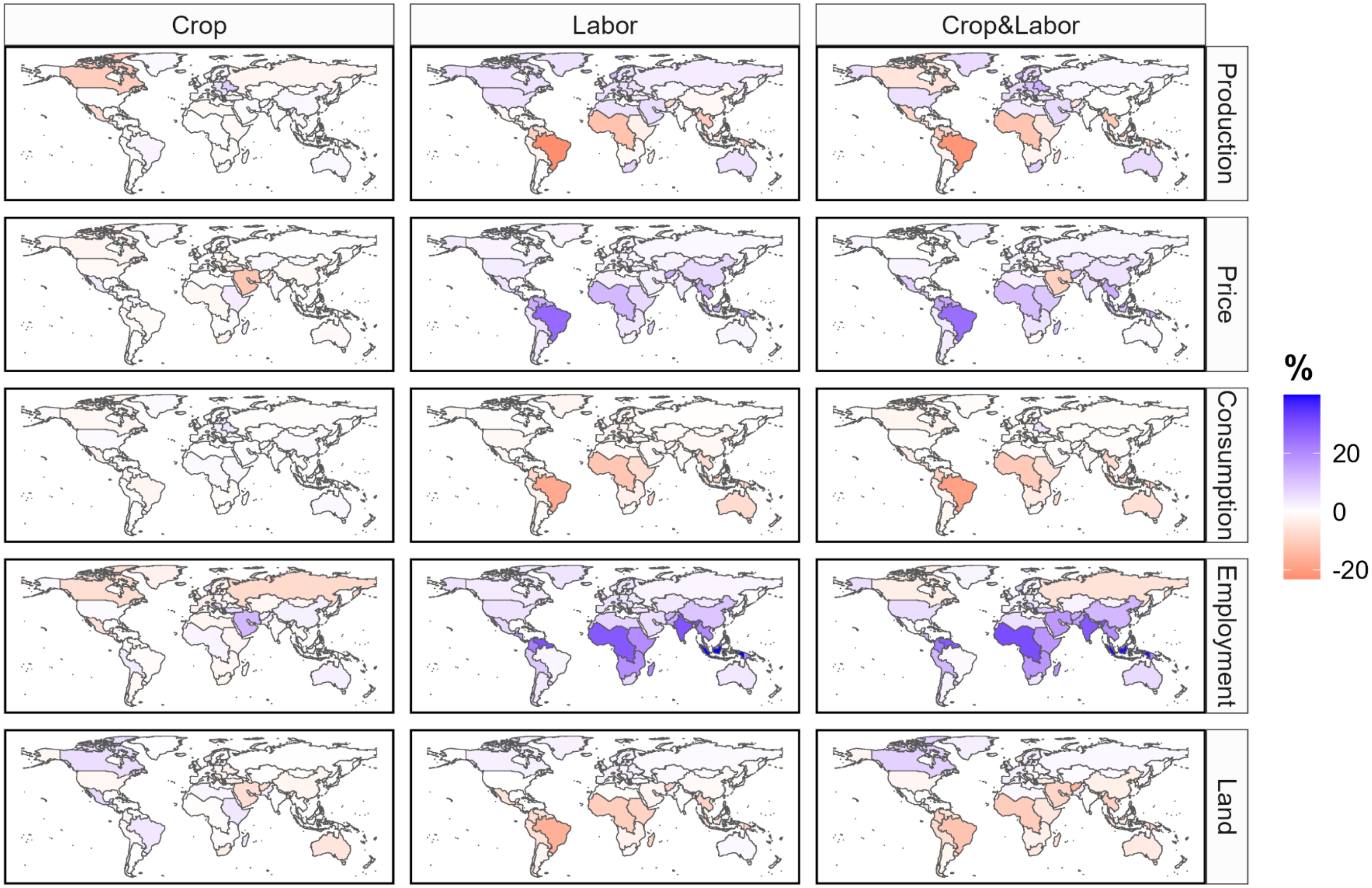

Fig.S7. Regional climate impact (%) on the other crops market in the Mild scenario, 2100. Data source: GCAM results

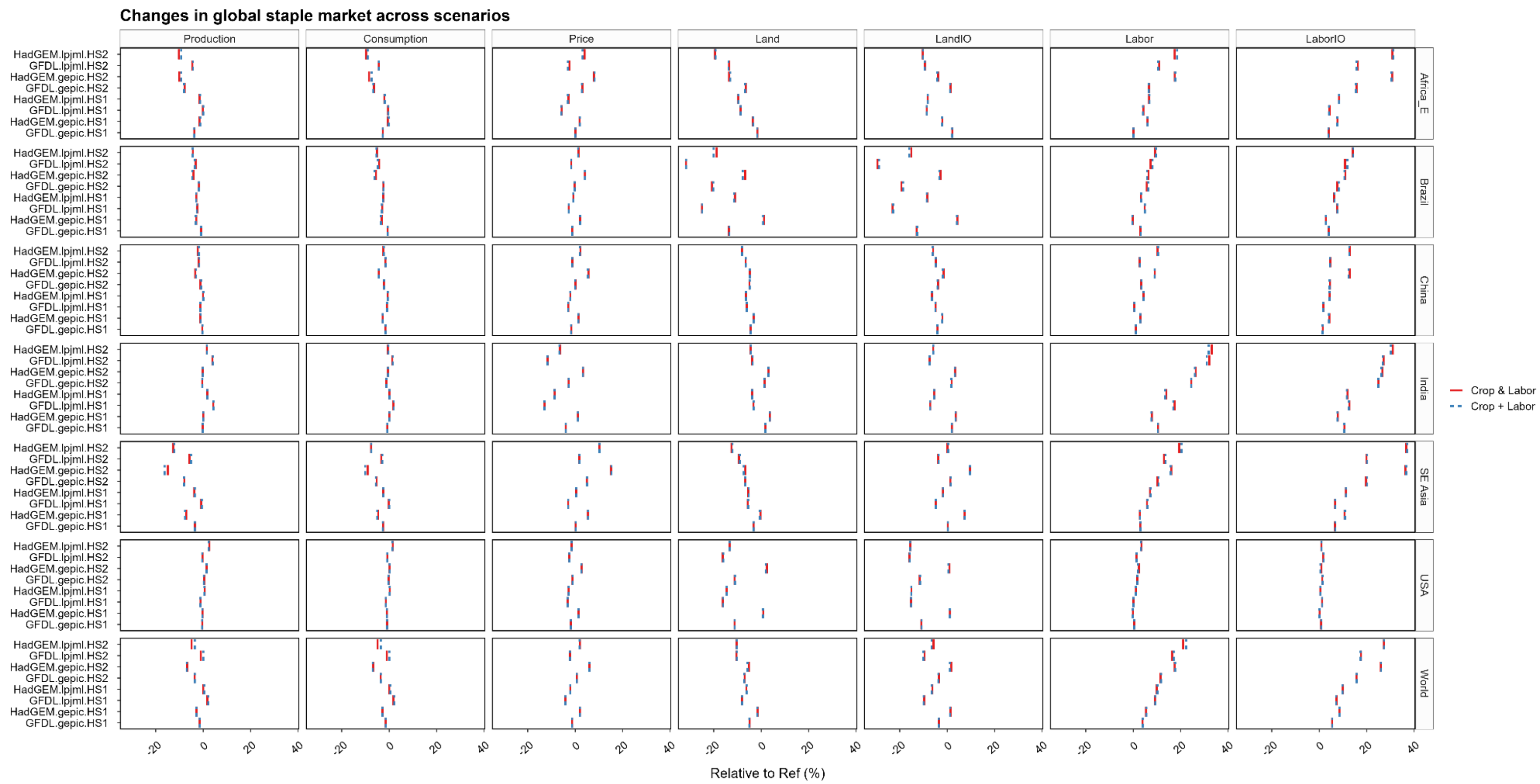

Fig. S8. Climate impact on agriculture across scenarios for selected GCAM regions. **Crop & Labor** denotes $\Delta\mathit{Combined}$, while **Crop + Labor** denotes the simple addition of $\Delta\mathit{Labor}^*$(Labor-only) and $\Delta\mathit{Crop}$ (Crop-only). HS1 and HS2 denote low and high labor-heat responses, respectively. LandIO and LaborIO denote the input-output coefficient of land and labor and are the reverse of crop yield and labor productivity. Source: GCAM outcomes.

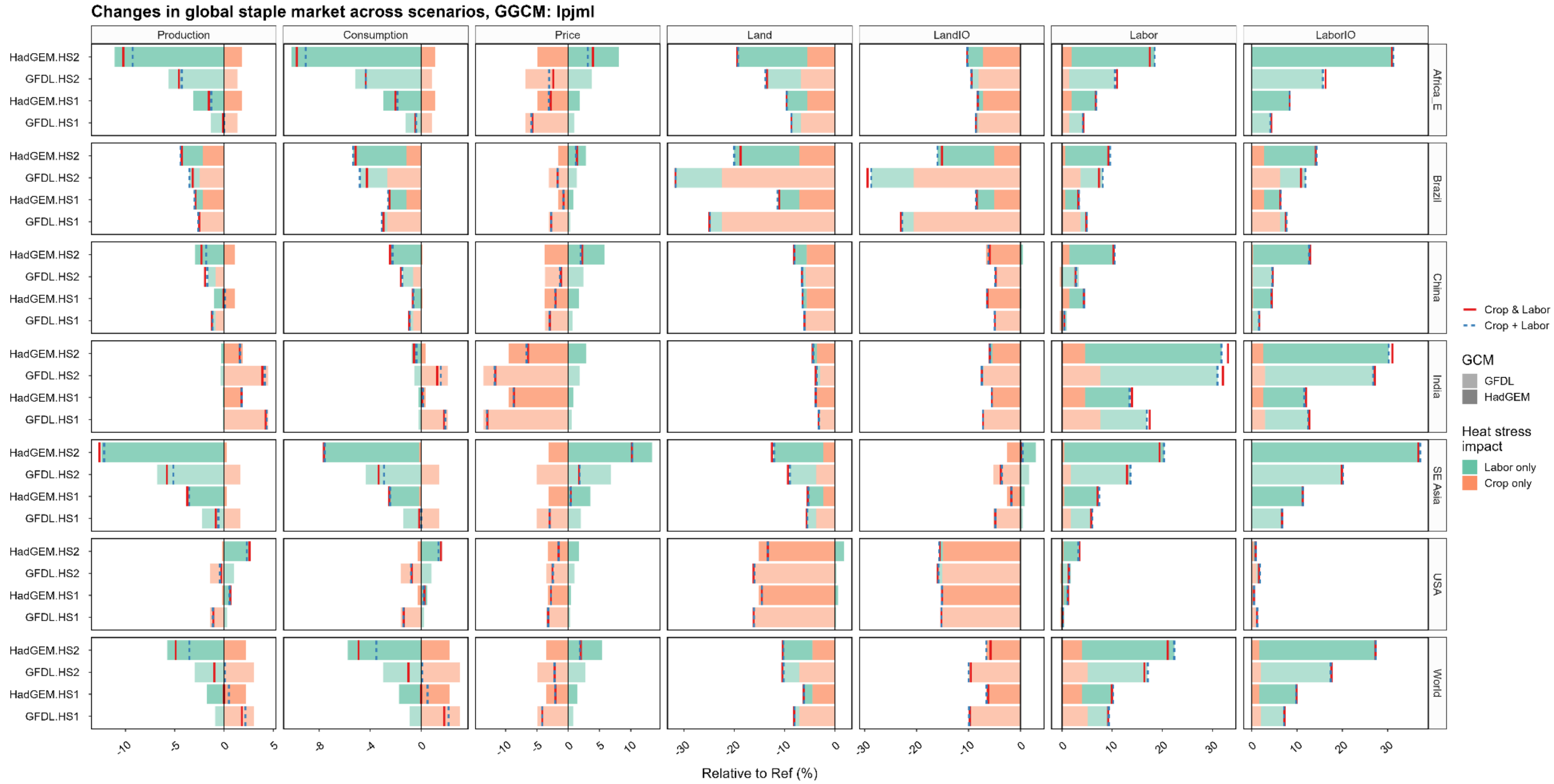

Fig.S9. Global staple crop market response with crop yield response from LPJmL for selected GCAM regions. HS1 and HS2 denote low and high labor-heat responses, respectively. LandIO and LaborIO denote the input-output coefficient of land and labor and are the reverse of crop yield and labor productivity. Source: GCAM outcomes.

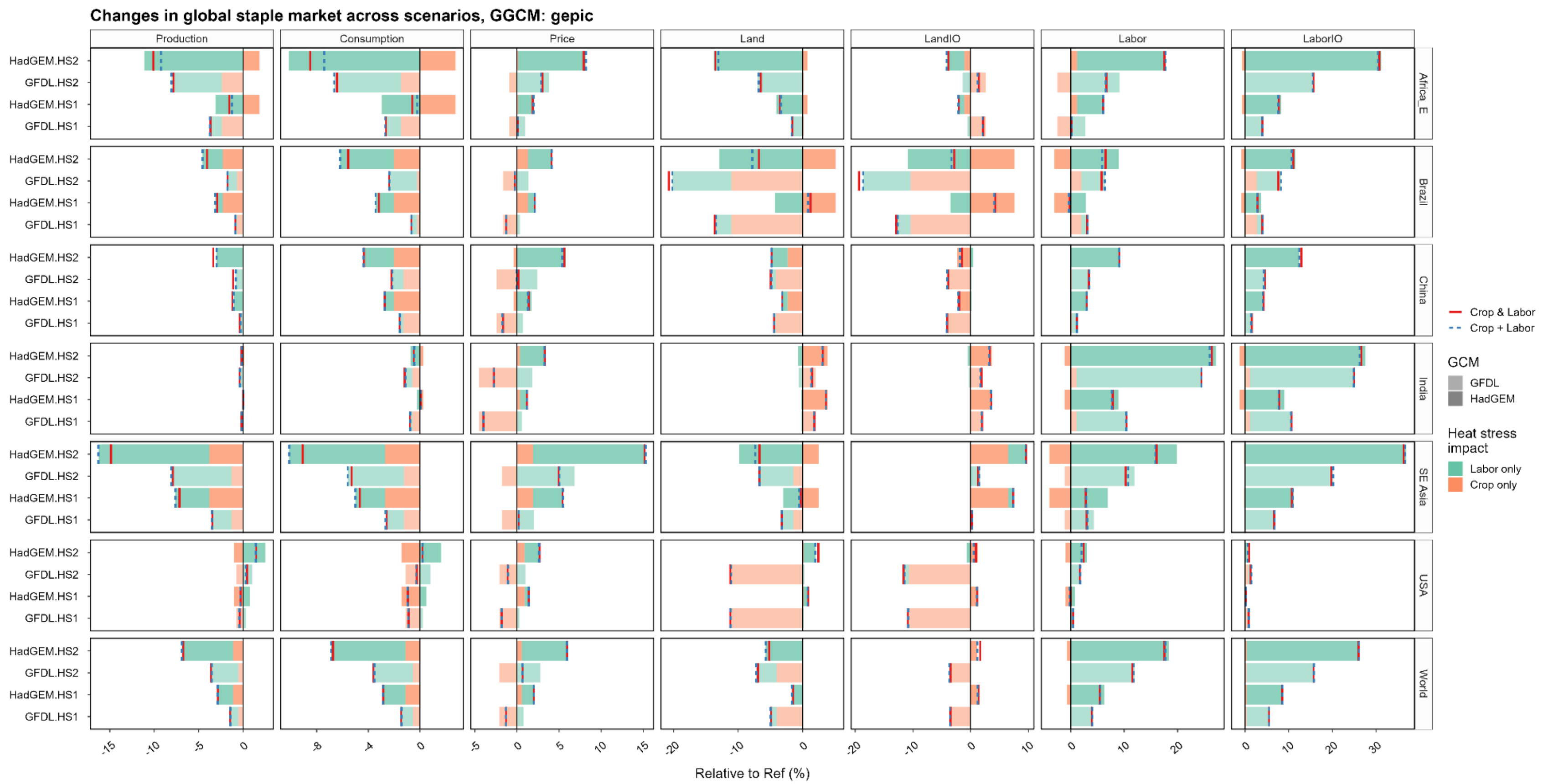

Fig.S10. Global staple crop market response with crop yield response from GEPIC for selected GCAM regions. HS1 and HS2 denote low and high labor-heat responses, respectively. LandIO and LaborIO denote the input-output coefficient of land and labor and are the reverse of crop yield and labor productivity. Source: GCAM outcomes.

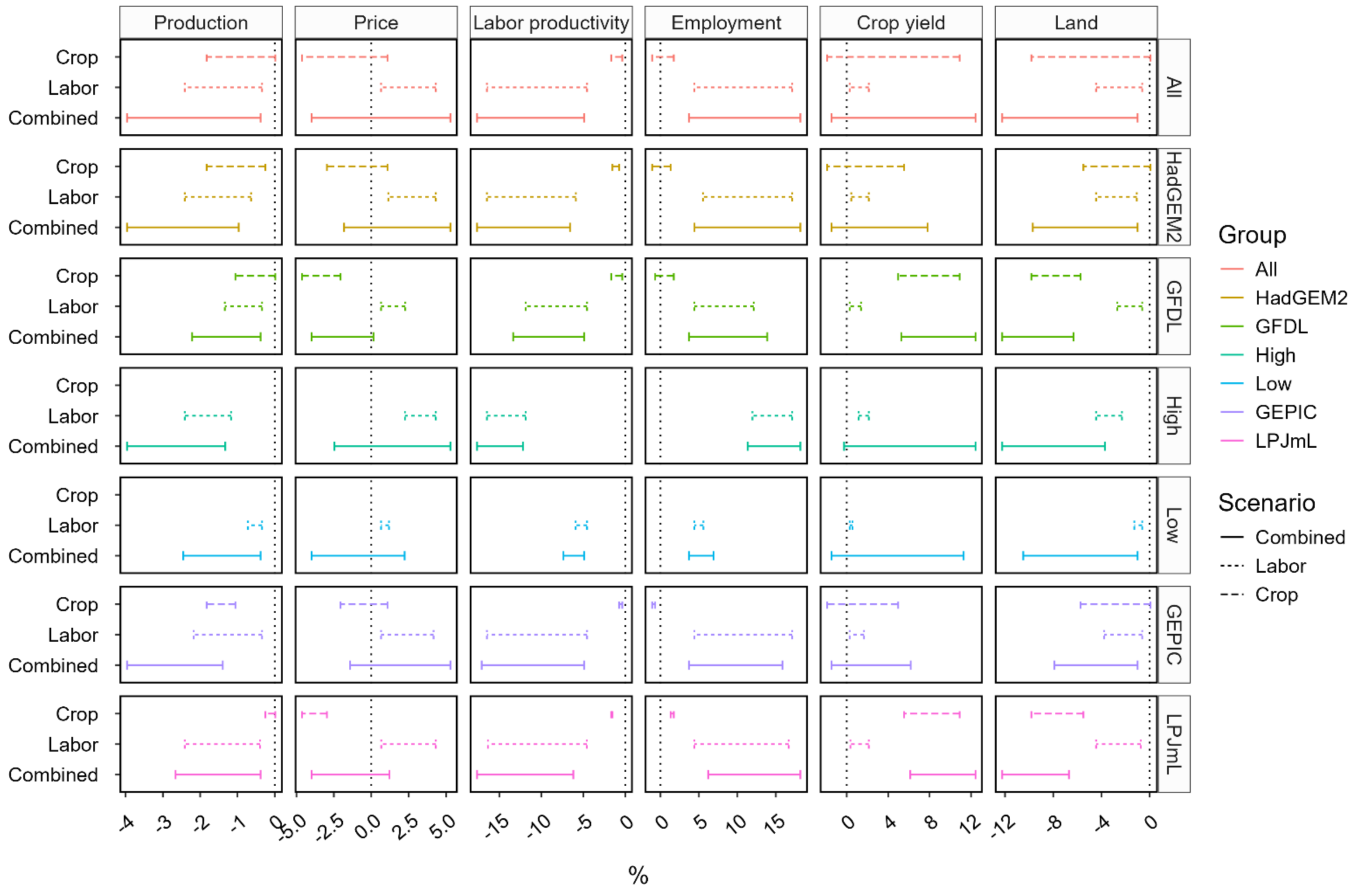

Fig.S11. Range of climate impact (%) on key crops across experiments and scenarios under RCP 6.0. Source: GCAM outcomes.

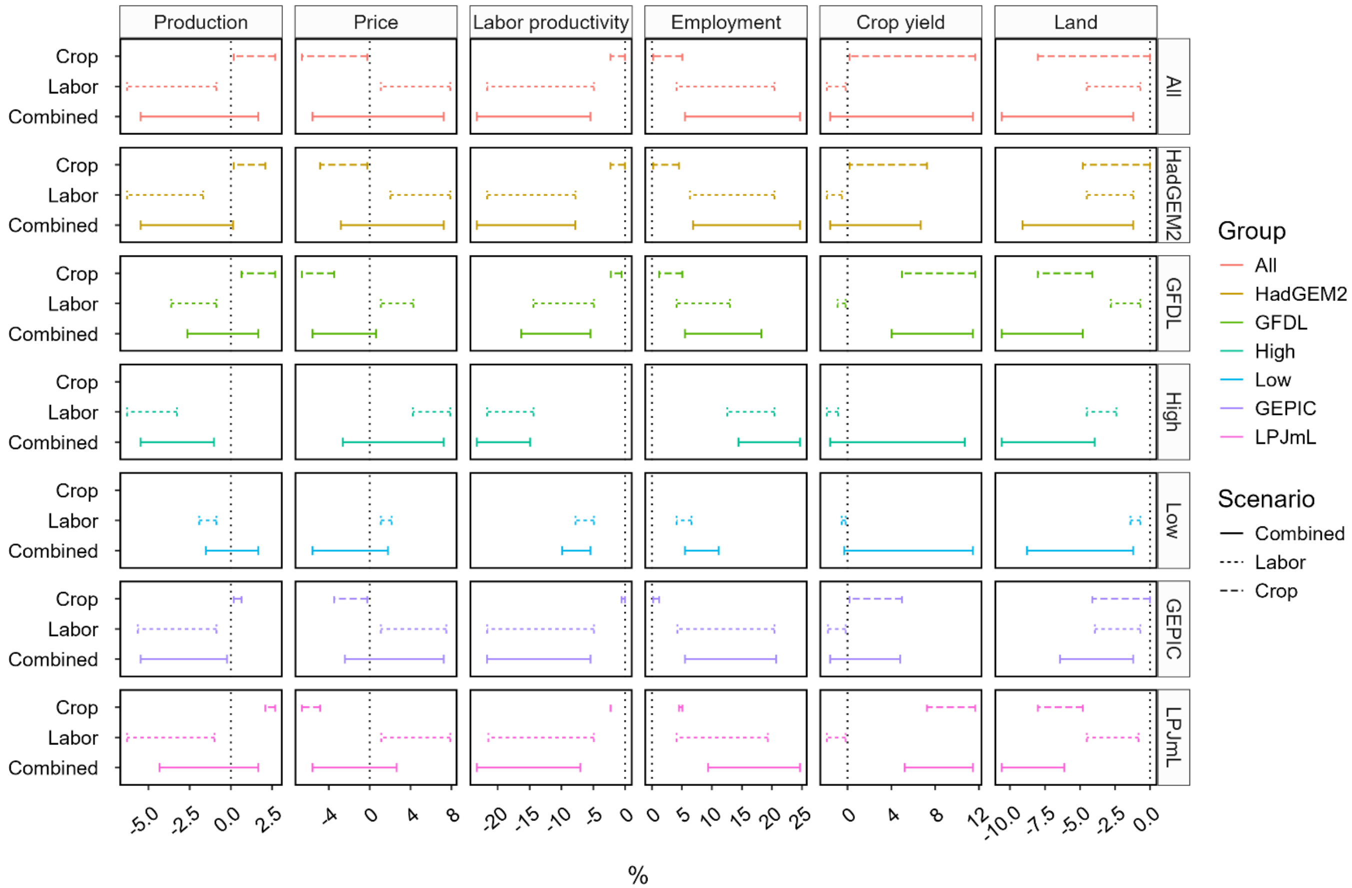

Fig.S12. Range of climate impact (%) on other crops across experiments and scenarios under RCP 6.0. Source: GCAM outcomes.

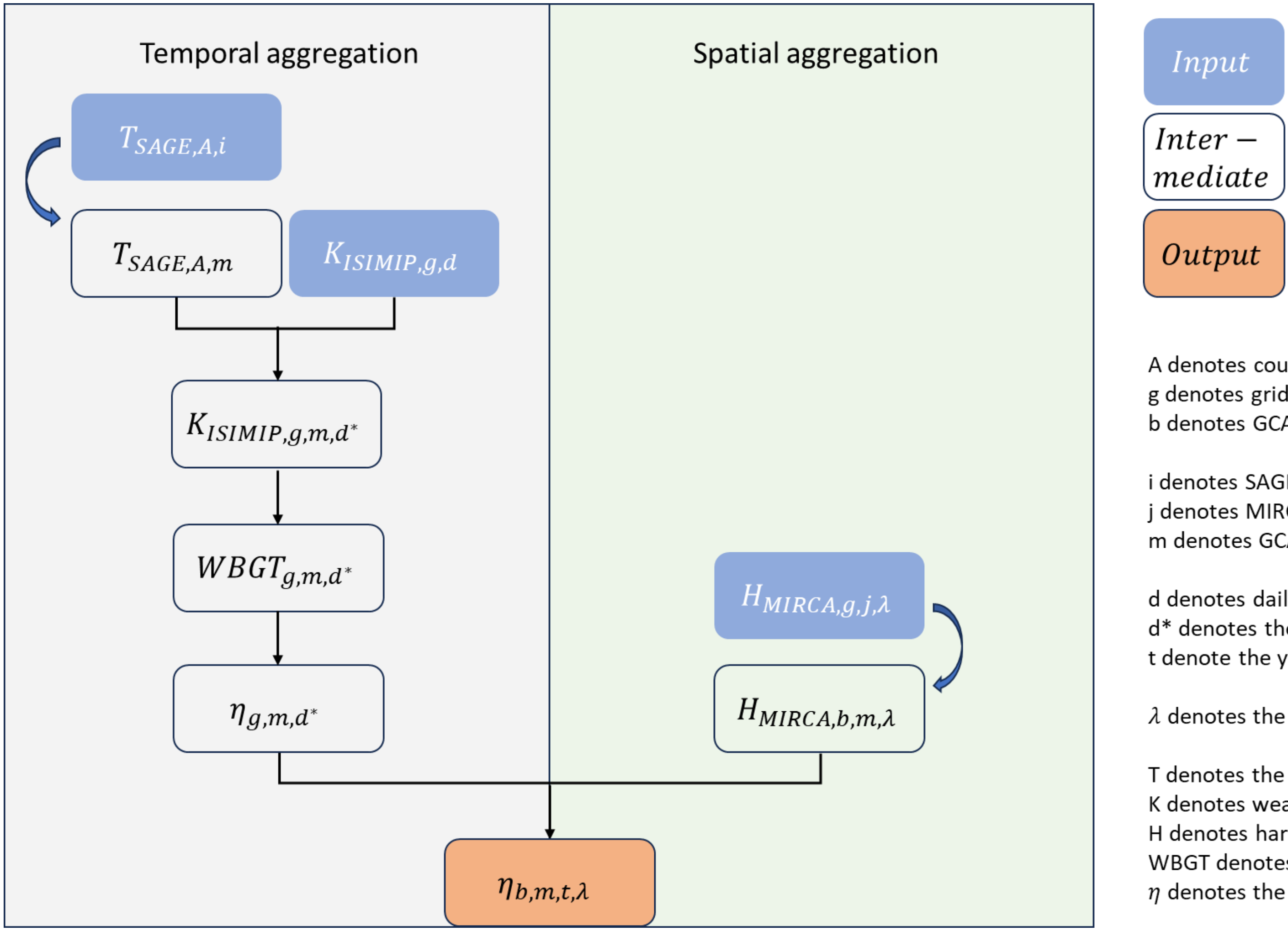

A denotes countries
g denotes grid-level
b denotes GCAM water basin

i denotes SAGE commodities
j denotes MIRCA commodities
m denotes GCAM commodities

d denotes daily level
d* denotes the crop days
t denote the year

λ denotes the irrigation practice

T denotes the crop calendar
K denotes weather input
H denotes harvested area
WBGT denotes the heat stress index
η denotes the labor productivity

Fig. S13. **Schematic** of translating weather input to labor productivity loss in GCAM.

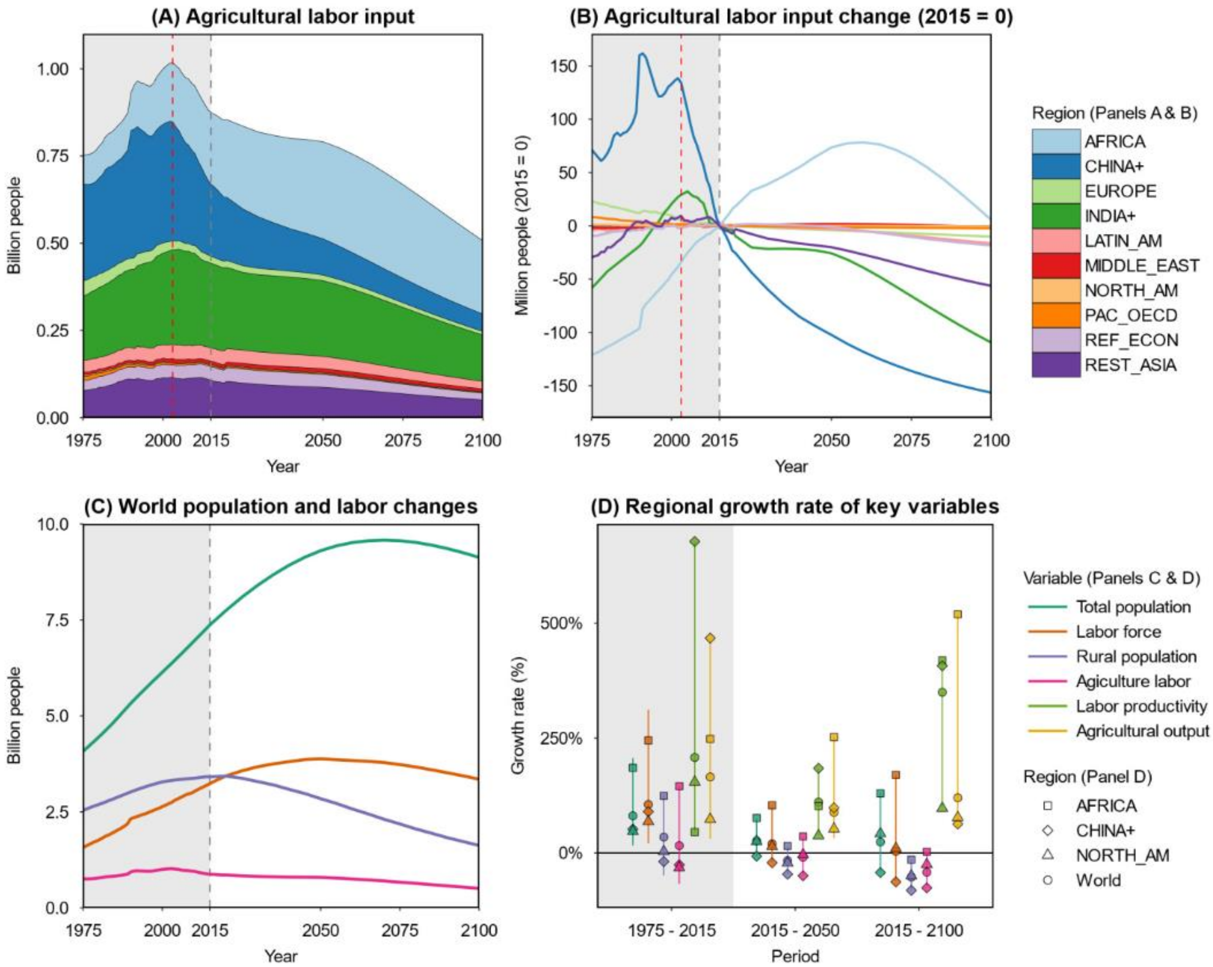

Fig.S14. Historical trends and future projections (Evolving scenario) of agricultural labor-related metrics. Panel (A) presents agricultural labor input by region (stacked areas), and Panel (B) shows the corresponding changes (lines) over time relative to 2015. Panel (C) shows changes in population and labor-related metrics at the world level. Panel (D) shows the growth rate of key variables by region and period. The point-range plots show values for key regions (shape of the point) and R10 region ranges (whiskers). Vertical dotted lines, where applicable, highlight 2003 (red) and 2015 (gray). Data from 1975 to 2015 (gray background areas) are historical observations compiled based on USDA and ILO data (Methods). Data after 2015 are projections from the SSP database (population and labor force) or the “Evolving” scenario (agricultural labor, labor productivity, and value output) in the current study (GCAM). The agricultural labor data presented labor in the primary crop, livestock, and forestry production but did not include labor in the fishery sector (3% globally). Source: Sheng et al (2024); **Copyright pending.**

S3. Supplementary Tables

Table S1. Summary of literature estimating climate impact and socio-economic consequences

Study	**Group**	**Response**	**Time**	**Climate**	**Method**
Zhao et al. (2017)[14]	Crop	Crop yield	Historical and future	Observed; 4 RCPs	Grid-based & point-based simulations, field experiments, Statistical regressions
Nelson et al. (2014)[15]	Crop	Agriculture market response	Future: 2050	RCP 8.5	CGE & PE models
Zhao et al. (2021)[16]	Crop	Agriculture market response	Future: 2050	RCP 8.5	PE: GCAM
Kjellstrom et al (2009a)[17]	Labor	Labor productivity	Historical	Observed	WBGT + Exposure function
Kjellstrom et al (2009b)[18]	Labor	Labor productivity	Historical and future	A2 & B2 from IPCC	WBGT + Exposure function
Dunne et al. (2013)[3]	Labor	Labor productivity	Future: 2050	RCP 8.5	WBGT + Exposure function
Somanathan et al. (2021)[19]	Labor	Manufacturing output	Historical: 1998-2009	Observed	Empirical estimates
Orlov et al. (2020)[20]	Labor	GDP	Future: 2100	RCP 8.5	CGE: GRACE
Matsumoto et al. (2021)[21]	Labor	GDP	Future: 2100	RCP 8.5	CGE: EPPA
Zivin and Neidell (2014)[22]	Labor	Labor supply	Historical: 2003-2006	observed	Empirical, regression
Lima et al. (2021)[23]	Crop & Labor	Agriculture market response	Static	+3C global warming	CGE: GTAP
Orlov et al. (2024)[24]	Crop & Labor	Agriculture market response	Static	RCP 7.0	CGE: GRACE

Table S2. Experiments and scenarios

Metric	Baseline	Experiment	Estimate
ΔCrop	**NoCC**	**Crop-only**: HadGEM2_GEPIC	C_HadGEM2_GEPIC, **Severe**
ΔCrop	**NoCC**	**Crop-only**: HadGEM2_LPJmL	C_HadGEM2_ LPJmL
ΔCrop	**NoCC**	**Crop-only**: GFDL_GEPIC	C_GFDL_GEPIC, **Mild**
ΔCrop	**NoCC**	**Crop-only**: GFDL_LPJmL	C_GFDL_ LPJmL
ΔLabor	**Crop**: HadGEM2_GEPIC	**Crop&Labor**: HadGEM2_GEPIC_High	L_HadGEM2_GEPIC_High, **Severe**
ΔLabor	**Crop**: HadGEM2_LPJmL	**Crop&Labor**: HadGEM2_LPJmL_High	L_HadGEM2_LPJmL_High
ΔLabor	**Crop**: GFDL_GEPIC	**Crop&Labor**: GFDL_GEPIC_High	L_GFDL_GEPIC_High
ΔLabor	**Crop**: GFDL_LPJmL	**Crop&Labor**: GFDL_ LPJmL_High	L_GFDL_ LPJmL_High
ΔLabor	**Crop**: HadGEM2_GEPIC	**Crop&Labor**: HadGEM2_GEPIC_Low	L_HadGEM2_GEPIC_Low
ΔLabor	**Crop**: HadGEM2_LPJmL	**Crop&Labor**: HadGEM2_LPJmL_Low	L_HadGEM2_LPJmL_Low
ΔLabor	**Crop**: GFDL_GEPIC	**Crop&Labor**: GFDL_GEPIC_Low	L_GFDL_GEPIC_Low, **Mild**
ΔLabor	**Crop**: GFDL_LPJmL	**Crop&Labor**: GFDL_ LPJmL_Low	L_GFDL_ LPJmL_Low
ΔLabor*	**NoCC**	**Labor-only**: HadGEM2_High	L*_HadGEM2_GEPIC
ΔLabor*	**NoCC**	**Labor-only**: HadGEM2_Low	L*_HadGEM2_ LPJmL
ΔLabor*	**NoCC**	**Labor-only**: GFDL_High	L*_GFDL_GEPIC
ΔLabor*	**NoCC**	**Labor-only**: GFDL_Low	L*_GFDL_ LPJmL
ΔCombined	**NoCC**	**Crop&Labor**: HadGEM2_GEPIC_High	CL_HadGEM2_GEPIC_High, **Severe**
ΔCombined	**NoCC**	**Crop&Labor**: HadGEM2_LPJmL_High	CL_HadGEM2_LPJmL_High
ΔCombined	**NoCC**	**Crop&Labor**: GFDL_GEPIC_High	CL_GFDL_GEPIC_High
ΔCombined	**NoCC**	**Crop&Labor**: GFDL_ LPJmL_High	CL_GFDL_ LPJmL_High
ΔCombined	**NoCC**	**Crop&Labor**: HadGEM2_GEPIC_Low	CL_HadGEM2_GEPIC_Low
ΔCombined	**NoCC**	**Crop&Labor**: HadGEM2_LPJmL_Low	CL_HadGEM2_LPJmL_Low
ΔCombined	**NoCC**	**Crop&Labor**: GFDL_GEPIC_Low	CL_GFDL_GEPIC_Low, **Mild**
ΔCombined	**NoCC**	**Crop&Labor**: GFDL_ LPJmL_Low	CL_GFDL_ LPJmL_Low

Table S3. MIRCA sector mapping to GCAM sector

GCAM crop	**MIRCA crop**
Corn	Corn
FiberCrop	Cotton
FodderGrass	Fodder grasses
Fruits	Citrus, Date palm, Grapes
Legumes	Pulses
MiscCrop	Coffee, Cocoa, Others annual, Others perennial
NutsSeeds	Groundnuts
OilCrop	Sunflower, Rapeseed
OilPalm	Oil palm
OtherGrain	Barley, Rye, Millet, Sorghum
Rice	Rice
RootTuber	Potatoes, Cassava
Soybean	Soybeans
SugarCrop	Sugar cane, Sugar beet
Wheat	Wheat

Table S4. SAGE sector mapping to GCAM sector

GCAM crop	**SAGE crop**
Corn	maize
FiberCrop	cotton, other(jute)
Fruits	banana
Legumes	pulses
MiscCrop	other(tobacco, multiple)
NutsSeeds	groundnuts
OilCrop	rapeseed, sunflower, other(castor, sesame, mustard)
OtherGrain	barley, millet, oats, rye, sorghum
Rice	rice
RootTuber	potatoes, cassava, yams, sweet.potatoes
Soybean	soybeans
SugarCrop	sugarbeets, sugarcane
Vegetables	other(onions, vegetables, tomato)
Wheat	wheat

Table S5. GCAM crop grouping for reporting

GCAM crop	**Grouping with Key crops**
Corn	Key
FiberCrop	Other crops
Fruits	Other crops
Legumes	Other crops
MiscCrop	Other crops
NutsSeeds	Other crops
OilCrop	Other crops
OtherGrain	Other crops
Rice	Key
RootTuber	Other crops
Soybean	Key
SugarCrop	Other crops
Vegetables	Other crops
Wheat	Key

Table S6. Regional mapping between GCAM regions and IPCC R10 regions

GCAM regions	IPCC R10 region
Africa_Eastern	Africa
Africa_Northern	
Africa_Southern	
Africa_Western	
South Africa	
China	China
Taiwan	
EU-12	Europe
EU-15	
Europe_Eastern	
Europe_Non_EU	
European Free Trade Association	
India	South Asia
Pakistan	
South Asia	
Argentina	Latin America
Brazil	
Central America and Caribbean	
Colombia	
Mexico	
South America_Northern	
South America_Southern	
Middle East	Middle East
Canada	North America
USA	
Australia_NZ	Pacific OECD
Japan	
South Korea	
Central Asia	Reforming economies
Russia	
Indonesia	Southeast Asia
Southeast Asia	

References

1. Sacks, W. J., Deryng, D., Foley, J. A. & Ramankutty, N. Crop planting dates: an analysis of global patterns. *Glob. Ecol. Biogeogr.* **19**, 607–620 (2010).
2. Davies-Jones, R. An Efficient and Accurate Method for Computing the Wet-Bulb Temperature along Pseudoadiabats. *Mon. Weather Rev.* **136**, 2764–2785 (2008).
3. Dunne, J. P., Stouffer, R. J. & John, J. G. Reductions in labour capacity from heat stress under climate warming. *Nat. Clim. Change* **3**, 563–566 (2013).
4. Matsumoto, K. Climate change impacts on socioeconomic activities through labor productivity changes considering interactions between socioeconomic and climate systems. *J. Clean. Prod.* **216**, 528–541 (2019).
5. Portmann, F. T., Siebert, S. & Döll, P. MIRCA2000—Global monthly irrigated and rainfed crop areas around the year 2000: A new high-resolution data set for agricultural and hydrological modeling. *Glob. Biogeochem. Cycles* **24**, (2010).
6. Ahsan, H., Khan, Z., Snyder, A., Kyle, P. & Vernon, C. osiris: An R package to process climate impacts on agricultural yields for the Global Change Analysis Model. *J. Open Source Softw.* **8**, 5226 (2023).
7. Edmonds, J. A., Link, R., Waldhoff, S. T. & Cui, R. A global food demand model for the assessment of complex human-earth systems. *Clim. Change Econ.* **08**, 1750012 (2017).
8. Sheng, D. *et al.* Agroeconomic and environmental implications of future labor market evolution. Preprint at https://doi.org/10.21203/rs.3.rs-4259856/v1 (2024).
9. Kc, S. & Lutz, W. The human core of the shared socioeconomic pathways: Population scenarios by age, sex and level of education for all countries to 2100. *Glob. Environ. Change* **42**, 181–192 (2017).
10. O’Neill, B. C. *et al.* The roads ahead: Narratives for shared socioeconomic pathways describing world futures in the 21st century. *Glob. Environ. Change* **42**, 169–180 (2017).
11. *World Agriculture towards 2030/2050: The 2012 Revision*. (2012). doi:10.22004/ag.econ.288998.

12. Alexandratos, N. *et al.* World agriculture: towards 2030/2050. Interim report. Prospects for food, nutrition, agriculture and major commodity groups. (2006).

13. Roson, R. & Sartori, M. Estimation of Climate Change Damage Functions for 140 Regions in the GTAP 9 Data Base. *J. Glob. Econ. Anal.* **1**, 78–115 (2016).

14. Zhao, C. *et al.* Temperature increase reduces global yields of major crops in four independent estimates. *Proc. Natl. Acad. Sci.* **114**, 9326–9331 (2017).

15. Nelson, G. C. *et al.* Climate change effects on agriculture: Economic responses to biophysical shocks. *Proc. Natl. Acad. Sci.* **111**, 3274–3279 (2014).

16. Zhao, X. *et al.* Global agricultural responses to interannual climate and biophysical variability. *Environ. Res. Lett.* **16**, 104037 (2021).

17. Kjellstrom, T., Holmer, I. & Lemke, B. Workplace heat stress, health and productivity – an increasing challenge for low and middle-income countries during climate change. *Glob. Health Action* **2**, 2047 (2009).

18. Kjellstrom, T., Kovats, R. S., Lloyd, S. J., Holt, T. & Tol, R. S. J. The Direct Impact of Climate Change on Regional Labor Productivity. *Arch. Environ. Occup. Health* **64**, 217–227 (2009).

19. Somanathan, E., Somanathan, R., Sudarshan, A. & Tewari, M. The Impact of Temperature on Productivity and Labor Supply: Evidence from Indian Manufacturing. *J. Polit. Econ.* **129**, 1797–1827 (2021).

20. Orlov, A., Sillmann, J., Aunan, K., Kjellstrom, T. & Aaheim, A. Economic costs of heat-induced reductions in worker productivity due to global warming. *Glob. Environ. Change* **63**, 102087 (2020).

21. Matsumoto, K., Tachiiri, K. & Su, X. Heat stress, labor productivity, and economic impacts: analysis of climate change impacts using two-way coupled modeling. *Environ. Res. Commun.* **3**, 125001 (2021).

22. Zivin, J. G. & Neidell, M. Temperature and the Allocation of Time: Implications for Climate Change. 1–26 (2014).

23. Lima, C. Z. de *et al.* Heat stress on agricultural workers exacerbates crop impacts of climate change. *Environ. Res. Lett.* **16**, 044020 (2021).

24. Orlov, A. *et al.* Human heat stress could offset potential economic benefits of CO2 fertilization in crop production under a high-emissions scenario. *One Earth* **7**, 1250–1265 (2024).